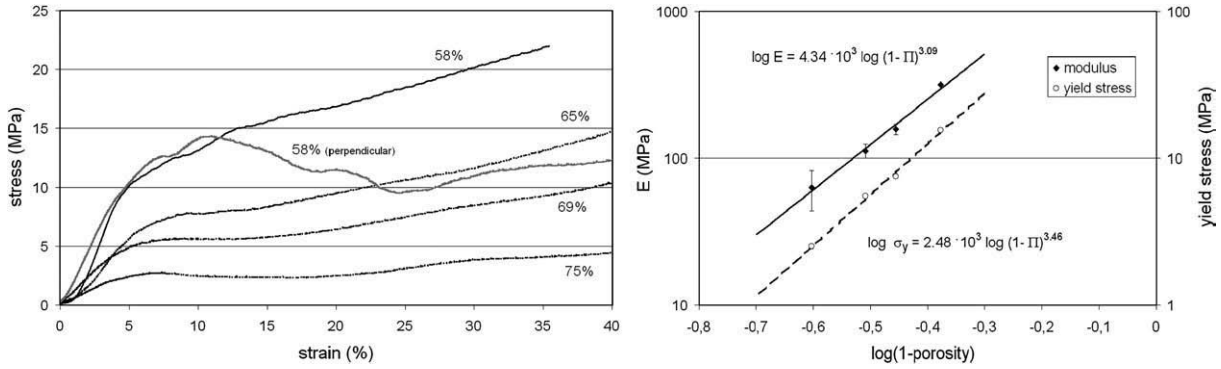

Fig. 3. Left: stress–strain diagram of the cubic scaffolds tested under compression. Right: log–log plot of Young's modulus and yield stress vs. polymer volume fraction.

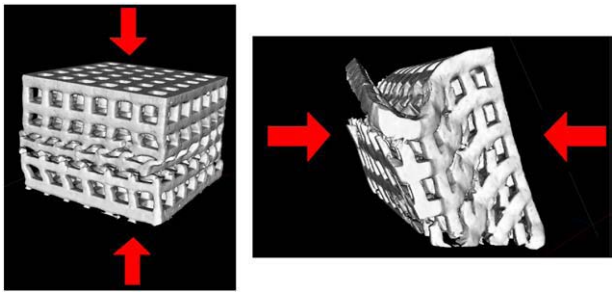

Fig. 4. Scaffolds compressed with 450 N (approximately 22 MPa) in the building direction (left) or perpendicular to the building direction (right).

The scaffolds were tested in compression in the building direction of the stereolithography process. As depicted in Fig. 3 all scaffolds show similar stress–strain profiles. After linear elastic behaviour, the specimens yield at 5–7% strain. The yield point can be determined by intersection tangents to the curve. This yielding corresponds to the collapse of one row of pillars in the construct as depicted in Fig. 4 (left). After this yield point, the stress slowly increases as following rows collapse. The lowest-porosity scaffold was also tested perpendicular to the building direction; this showed deviating mechanical behaviour.

Fig. 4 demonstrates the difference in deformation. Apparently, connections within a layer are stronger than connections between different layers.

The modulus and yield stress are plotted against the polymer volume fraction (1-porosity) in a log–log plot in Fig. 3 (right). Both could well be fitted (R^2=0.99) with a power law. The intercept 4.3 GPa for the modulus corresponds to the bulk compressive modulus of densely crosslinked PDLLA.

These porous scaffolds have superior mechanical properties when compared to scaffolds made using traditional polymer-processing techniques, such as porogen leaching or gas foaming. Photo-polymerised, salt-leached PDLLA scaffolds of 75% porosity show a compressive modulus of 23 MPa, compared to 63 MPa for the SLA-built PDLLA structure of 75% porosity. Stress at 5% strain (near the yield point) is 0.6 vs. 2.4 MPa. Values reported for the modulus of trabecular bone vary from 10 to 1000 MPa [1], which can be attained with SLA-built PDLLA scaffolds by varying the porosity.

Conclusion

A stereolithography resin based on poly(d,l-lactide) was developed and used to build highly regular, pre-designed, biodegradable scaffolds with varying porosities. Their mechanical properties strongly depend on the porosity, and can be adjusted in a predictable way.

Acknowledgement

We would like to acknowledge the European Union for financial support through the STEPS project (Contract n° NMP3-CT-2005-500465).

Reference

[1] A.H. Burstein, D.T. Reilly, M. Martens, J. Bone Joint Surg. 58 (1976) 82–86.

doi:10.1016/j.jconrel.2008.09.066

Preparation of porous poly(trimethylene carbonate) structures for controlled release applications using high pressure CO_2

S.P. Nalawade[a], D. Westerman[b], G. Leeke[b], R.C.D. Santos[b], D.W. Grijpma[a,*], J. Feijen[a]

[a] *Institute for Biomedical Technology (BMTI), Department of Polymer Chemistry and Biomaterials, University of Twente, P.O. Box 217, 7500 AE Enschede, The Netherlands*

[b] *Department of Chemical Engineering, University of Birmingham, Edgbaston, Birmingham, B15 2TT, UK*

Abstract

Porous poly(trimethylene carbonate) structures can readily be prepared using high pressure CO_2. Differences in CO_2 solubility in the polymer matrix at the different processing temperatures and pressures lead to different pore morphologies upon depressurization. Furthermore, crystallization of the initially amorphous polymer leads to stable porous structures. This variation in pore structure can be used to tailor polymer matrix degradation rates and drug release profiles.

Introduction

Poly(trimethylene carbonate) (PTMC) is an amorphous, flexible polymer that degrades *in vivo* by surface erosion without the release of acidic compounds [1]. This makes the polymer most suited for drug delivery applications. By preparing a porous polymeric structure, its degradation rate and the release profiles of drugs, proteins, growth factors or DNA can be controlled by adjusting pore sizes and porosities [2,3].

High pressure carbon dioxide (CO_2) can be used as a polymer processing aid and as a porogen. Its inert nature and gas-like diffusivity and liquid-like density at and above supercritical conditions (31 °C and 7.38 MPa) are major advantages in its use. In general, pressure and temperature determine the amount of CO_2 that can be dissolved in a polymer matrix. Upon depressurization, supersaturation of the dissolved CO_2 induces nucleation of CO_2 bubbles in the matrix that can result in the formation of a porous polymer structure. Porous materials with variable pore characteristics can be prepared by adjusting the temperature and CO_2 pressure.

Experimental methods

PTMC was synthesized by ring opening polymerization of trimethylene carbonate at 130 °C for 3 days in an inert argon atmosphere. As catalyst 2×10^{-4} mol stannous octoate per mol monomer was employed. The prepared polymer was dissolved in chloroform, precipitated in a tenfold volume of ethanol and dried in vacuum. The PTMC polymer was compression moulded at 140 °C and cut into small sheets measuring $0.5 \times 5 \times 10$ mm^3. Foaming experiments were carried out in a 500 ml high pressure vessel. The vessel was charged with the polymer specimens and purged with CO_2. Subsequently, it was heated and pressurized to the desired temperature and pressure values. The samples were then allowed to saturate with high pressure CO_2 for at least 2 h. Finally, the vessel was depressurized to atmospheric pressure by rapidly releasing CO_2, thereby nucleating the formation of gas bubbles in the polymer samples. In other experiments, the samples were transferred to an oven heated to 70 °C immediately after depressurization and kept at this temperature for 2 min.

Nuclear magnetic resonance (NMR, Varian Inova 300 MHz) of polymer solutions in deuterated chloroform was employed to determine monomer conversion. Gel permeation chromatography (GPC, Viscotek equipped with a triple detector array) calibrated with narrow polystyrene standards was used to determine molecular weights of the polymer.

Differential calorimetry (DSC, Perkin Elmer Pyris 1) was operated at a heating rate of 10 °C/min to investigate the thermal characteristics of the materials in the first scan.

The foamed porous structures were cryogenically fractured, sputtered with gold and evaluated by scanning electron microscopy (SEM, JEOL).

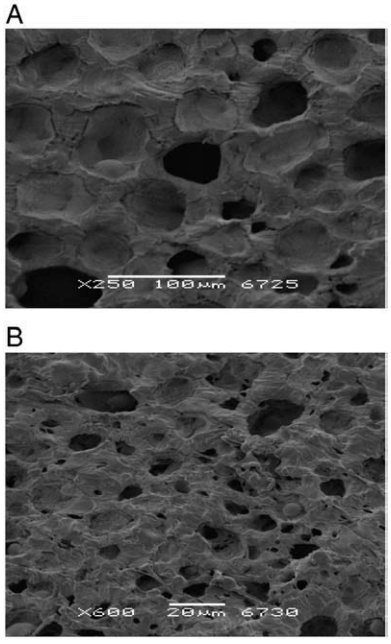

Fig. 1. SEM micrographs of PTMC subjected to different CO_2 pressures at 25 °C: A) P_{CO_2} = 6 MPa and B) P_{CO_2} = 12 MPa. The saturation time was t_s = 5 h and the depressurization time was t_d = 2 min.

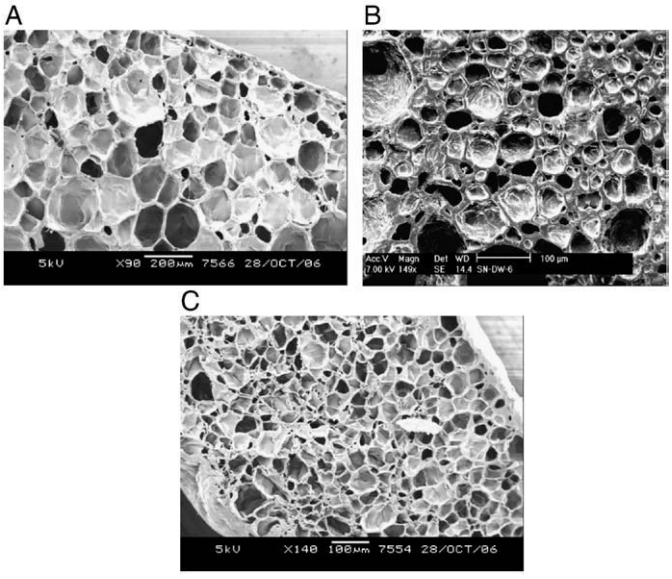

Fig. 2. SEM micrographs of PTMC subjected to different CO_2 pressures at 25 °C: A) P_{CO_2} = 6 MPa, B) P_{CO_2} = 12 MPa and C) P_{CO_2} = 17 MPa. The saturation time was t_s = 2 h, the depressurization time was t_d = 0.5 min, and the heating time at 70 °C immediately upon depressurization was t_h = 2 min.

Table 1
DSC analysis of PTMC specimens subjected to CO_2 at different temperatures and pressures

Polymer	T (oC)	CO_2 P (MPa)	T_g (oC)	T_m (oC)	ΔH_m (J/g)
PTMC	no CO_2	no CO_2	−14.2	–	–
PTMC	25	6	−14.9	35.3	12.1
PTMC	25	12	−14.0	35.5	12.3
PTMC	90	12	−16.6	–	–
PTMC	90	17	−17.0	–	–
PTMC	90	30	−16.4	34.8	13.6
PTMC	25+70[a]	6	−16.5	39.0	13.1
PTMC	25+70[a]	17	−16.8	40.1	18.6

[a] Immediately upon depressurization, the specimens were exposed to a temperature of 70°C for 2 min.

Results and discussion

Under the given experimental conditions, monomer conversions exceeded 99%. After purification, the number average and the weight average molecular weights were 420×10^3 and 560×10^3 g/mol, respectively. The synthesized PTMC was amorphous, with a low glass transition temperature of approximately −14 °C. First batch foaming experiments were conducted at a relatively low temperature of 25 °C. Specimens were subjected to CO_2 pressures of 6 and 12 MPa, and depressurized. Fig. 1 shows SEM micrographs of the resulting structures. Porous structures are obtained, in which the pore size decreases with increasing CO_2 pressure. At a higher CO_2 pressure, the amount of CO_2 dissolved in the polymer is higher. This leads to a higher degree of supersaturation, in which more and smaller pores are nucleated.

Although a porous structure is formed, the overall porosity is rather low. During depressurization of the dissolved CO_2, heat is absorbed, the polymer matrix cools, and pore growth is hindered. Increasing the foaming temperature to 90 °C does not yield better structures as CO_2 solubility is reduced at higher temperatures. If the polymer is exposed to a higher temperature immediately after conditioning and depressurization, more nucleated bubbles may grow to larger sizes due to lower viscosities of the polymer. Fig. 2 shows the resulting porous PTMC structures after saturation at different CO_2 pressures at 25 °C, followed by heating at 70 °C for 2 min immediately after depressurization. The figure shows that materials with high porosity and cell density could be prepared. As the solubility of CO_2 in the polymer is related to pressure, nucleation density increases and pore size decreases with pressure.

It is known that in amorphous crystallizable polymers, crystallization can be induced upon processing with high pressure CO_2 [4]. Table 1 shows such an effect for these PTMC foams. This crystallization aids in the stabilization of the pore structure, as these porous materials were found to be quite stable over prolonged time periods of up to 6 months.

Conclusions

High pressure CO_2 can be used to prepare microcellular PTMC foams. Materials with different pore sizes and densities can readily be prepared by

varying the temperatures and CO_2 pressures. Under certain processing conditions, crystallization could be induced in the initially amorphous polymer. This stabilizes the pore structure.

Acknowledgement

Financial support from EU project FP6-517070 (PROTEC) is greatly appreciated.

References

[1] A.P. Pego, et al., J. Biomed. Mater. Res. A 67 (2003) 1044–1054.
[2] D. Klose, et al., J. Pharmaceutics 314 (2006) 198–206.
[3] V. Lemair, J. Belair, P. Hildgen, Int. J. Pharm. 258 (2003) 95–107.
[4] Y.T. Shieh, Y.G. Lin, J. Appl. Polym. Sci. 87 (2003) 1144–1151.

doi:10.1016/j.jconrel.2008.09.067

Antimicrobial crosslinked polystyrene nanospheres for specialty multifunctional textile production

A.N. Nochos[a,b,*], S.M. Iconomopoulou[a], G.A. Voyiatzis[a]
[a] *FORTH/ICEHT, 18 Stadiou Str., P.O. Box 1414, GR-26504, Rio-Patras, Greece*
[b] *Department of Pharmacy, University of Patras, Greece*

Abstract

Antimicrobial crosslinked polystyrene nanospheres with controlled release characteristics were produced via a mini-emulsion polymerization technique and characterized by SEM and dynamic light scattering. Depending on the composition and the amount of the surfactant added, this method produced distinct nanosized (35–200 nm) beads. Uniform films of selected nanobeads that incorporated polypropylene were subsequently uniaxially drawn. The release profile of the antimicrobial agent was correlated with the induced molecular orientation of the polymer matrix revealed by polarized Raman spectroscopy.

Introduction

Over the past few decades there has been a constantly increasing concern about the health hazards arising during medical and other treatments from microbial infections. As a result, the means of shielding oneself against such threats need to be developed with one of the most popular being the production of antimicrobial textiles for usage inside the protective clothing, medical gauzes, sheets etc. For the production of such textiles two strategies are the most commonly employed. The first one deals with the coating of the antimicrobial on the final textile, while the second one concerns its incorporation into the compounding utilized for fiber production. The last strategy requires an antimicrobial preparation resistant to the high temperatures usually required for the production of synthetic fibers and if possible with controlled release characteristics for increased longevity of the desired antimicrobial efficacy of the final product. In a previous work, we had developed micron-sized polymeric beads loaded with antibacterial agents via suspension polymerization [1]. Although those beads exhibited controlled release characteristics, their size restricted the incorporation of the beads into textile fibers, usually having a diameter of about 15 μm. In an attempt to reduce the particle size to a desirable/optimum level, we utilized a mini-emulsion polymerization technique. More particularly, the present study describes the preparation of stable polymeric nanoparticles carrying triclosan, a widely used antimicrobial agent. The extremely low water solubility of the antimicrobial maximizes its retention in the emulsion's oil phase (polymer matrix) and the nanobeads developed can act as a 'storage cell' for the antimicrobial offering protection for the high temperatures involved in the spinning process. Moreover, varying the amount of divinyl benzene (DVB) allows control of the crosslinking density of the polymer and therefore control of triclosan's release rate. The nanoparticles were further incorporated by melt mixing into the polypropylene matrix that has been subsequently successfully uniaxially drawn. The induced molecular orientation constitutes an additional parameter for the antimicrobial agent release kinetics [2].

Experimental methods

The aqueous phase was created by mixing 51 ml of the deionized water with the surfactant sodium dodecyl sulfate (SDS) and $NaHCO_3$ at 40 °C using magnetic stirring for 30 min (10 ml of the water was saved for dissolving the initiator in a later stage). Styrene, DVB, hexadecane and triclosan, which compose the oil phase of the emulsion, were also mixed under magnetic stirring for a few minutes.

The oil phase was transferred into the aqueous one and subsequently the whole emulsion mixture was sonified (using an S30H Elmasonic sonication device) in an ice bath for 10 min in order to minimize the monomer-antimicrobial droplet size.

Finally, the emulsion containing flask was placed in an oil bath where it remained magnetically stirred and then heated to 80 °C, until the addition of potassium persulfate (KPS) solution initiated the polymerization reaction. The above reaction conditions were maintained overnight. It is worth noticing that different compositions of beads were synthesized in which the %DVB as well as the %triclosan was varied in order to investigate their effect on the release rate. Finally, the solid PS-DVB *X*%-triclosan *Y*% nanoparticles were isolated from the emulsion by freeze drying. Samples after freeze drying were analyzed by dynamic light scattering using a Malvern Zetasizer nano-ZS while a Leo Supra 35VP scanning electron microscope was utilized to conduct morphological characterization at the freeze dried material. For the release experiments, a known amount of nanoparticles was dispersed in 2 ml of ethanol solution and introduced into a dialysis bag (regenerated cellulose dialysis tubing) which was subsequently immersed in a known volume of the same solution. A Hitachi U-3000 UV–Vis spectrophotometer was utilized for the investigation of the release rate. Nanoparticle–polymer blends were produced by melt mixing the beads with PP at 200 °C for 10 min. Then, a final step of melt-pressing between teflon sheets was used to form the nanoparticle-loaded polymer uniform films. Those films were uniaxially drawn at various ratios using a home-made stretching element before being immersed into ethanol solutions for the investigation of the release rate of the entrapped antibacterial agent.

Results and discussion

Scanning electron microscopy imaging of all PS-DVB *X*%-triclosan *Y*% nanoparticles revealed distinct spherical particles with an overall smooth surface. Representative SEM images of the nanoparticles are illustrated in Fig. 1. In the case of PS-DVB 1%-triclosan 5% beads, that were synthesized with the addition of 0.3% w/v of surfactant their particle size appeared to be ~200 nm. A significant reduction in size was accomplished with the increase of SDS addition to a level of 2% w/v, in the case of synthesis of PS-DVB 2%-triclosan 10% beads. In the last case, SEM pictures revealed bead sizes of 35 nm which is in good agreement with the results of the DLS analysis.

The release profiles of the encapsulated antimicrobial agent from the various nanoparticle formulations showed a dependence upon the crosslinking density of the system, as expected. Specifically, in the case of the higher DVB-bearing formulations (with the same triclosan loading) a slower release rate was exhibited, attributed to the increase of the crosslinking density (Fig. 2).

Triclosan's release profiles from the nanoparticles incorporated in polypropylene films are depicted in Fig. 2. More precisely for the release study, samples, undrawn ($\lambda=1$) and after uniaxial drawing to $\lambda=6$, were immersed in 50% ethanol solutions and UV–Vis spectra were obtained from the solution at different time intervals. The release showed a direct dependence on the molecular orientation of the polymer film induced during uniaxial drawing suggesting another level of control over the release rate.

Conclusion

Polymeric nanoparticles loaded with triclosan were successfully synthesized. Those beads exhibit good release characteristics and more of that can be easily incorporated in polymeric matrixes like PP for the production of textile fibers. In addition, the nanoparticle containing matrixes were uniaxially drawn, a similar process to spinning. The molecular orientation as well as the synthesis offers interesting parameters to achieve controlled release and as a final step the production of antimicrobial fibers.

Acknowledgements

The financial support by the Operational Program of Western Greece/GSRT (PEP_DEL_19) is greatly acknowledged. The authors are also indebted